J Korean Radiol Soc 2008;58:97 - 104

Lesion Conspicuity of Hypoxic-ischemic Encephalopathy in Neonates: a Comparison of Various Magnetic Resonance Imaging Sequences[1]

Dae Wook Yeh, M.D., Hak Jin Kim, M.D.,Tae Un Kim, M.D., Sang Ook Nam, M.D.[2], Su Eun Park, M.D.[2]

Purpose: To determine which magnetic resonance (MR) imaging sequence demonstrates the highest lesion conspicuity for lesion detection in neonates with hypoxic-ischemic encephalopathy (HIE).

Materials and Methods: In 30 neonates with HIE, lesion conspicuity in different brain structures was retrospectively compared on T1-weighted images, T2-weighted images, fluid-attenuated inversion recovery images, and diffusion-weighted images (DWI). The brain structures were categorized as follows: cerebral cortex; cerebral white matter; deep gray matter; posterior limb of the internal capsule (PLIC); brain stem; and cerebellum.

Results: For the deep gray matter, T1-weighted imaging was superior to the other sequences in lesion detection of 9 of 14 patients (64.3%), whereas DWI was superior in only 4/14 patients (28.6%). For the cerebral cortex, T1- and DWI were similar in lesion conspicuity (5/13 patients and 6/13 patients, respectively). For the white matter, HIE lesions were most conspicuous on DWI in a majority of the study patients. Lesions were detected in the cerebral white matter in 16/20 patients (80.0%), lesions were detected in the PLIC in 11/12 patients (91.7%), lesions were detected in the corticospinal tract in the brain stem in 11/11 patients (100%) and lesions were detected in the cerebellar white matter in one patient (100%).

Conclusion: In neonates with HIE, white matter lesions are most conspicuous on DWI, whereas gray matter lesions tend to have greater conspicuity on T1-weighted images than on the other MR sequences.

Index words : Infant, newborn
Hypoxia-ischemia, brain
Magnetic resonance (MR)

In neonates and young children, global brain hypoxia-ischemia is a common mechanism of brain injury (1). Among all hypoxic-ischemic encephalopathy (HIE) cases, 15 - 20% of patients die during the neonatal period and 30% of those who survive suffer from neuro-developmental disorders, such as cerebral palsy and mental retardation (2). Clinical confirmation of ischemic damage is often difficult (3). Advances in neuroimaging have made a significant impact on HIE by demonstrating its pathology (4).

[1]Departments of Diagnostic Radiology and [2]Pediatrics, Pusan National University Hospital, Busan, South Korea
Received September 6, 2007 ; Accepted November 1, 2007
Address reprint requests to : Hak Jin Kim, M.D., Department of Diagnostic Radiology, Ami-dong 1 ga, Seo-gu, Busan, South Korea
Tel. 82-51-240-7354 Fax. 82-51-244-7534
E-mail: hakjink@pusan.ac.kr

However, the use of conventional magnetic resonance (MR) imaging techniques is known to be limited for the detection of the presence and extent of hypoxic-ischemic injury due to incomplete myelination and the high water content of the neonatal brain (5, 6). On diffusion-weighted imaging of neonates with HIE, underestimation of the extent of disease or false-negative results have been consistently reported (7 - 11). Therefore, all MR sequences are limited to some extent in their ability to depict HIE lesions. Furthermore, there is little available data regarding which sequence best depicts HIE lesions. The purpose of this study is to compare lesion conspicuity in neonates with HIE on various MR imaging sequences and to determine which sequence demonstrate the highest lesion conspicuity for lesion detection.

Materials and Methods

Subjects

From a review of our hospital database, we retrospectively identified neonates born after a gestational age of more than 35 weeks, i.e. near-term and term-born neonates, who had been examined with brain MR imaging between March 2002 and November 2006. The infants were selected if they had an apparent history of global hypoxic-ischemic injury and abnormalities that were seen on MR images.

The presence or absence of MR imaging abnormalities were determined by one radiologist based on the use of the following method. The MR images were compared with the MR images of neonates without brain abnormalities. Neonates without pathological changes seen at MR imaging were identified by using a keyword query in our picture archiving and communication system for the period from December 2005 to November 2006. The selected keyword was "no remarkable abnormal finding". MR examinations were selected consecutively from November 2006 back to December 2005 until the target numbers of 10 patients were reached. MR examinations in these control subjects were performed for an analysis of neonates that were suspected of having a brain tumor or congenital abnormality. One radiologist evaluated the MR images in these neonates, and the images disclosed a normal degree of myelination and no pathological changes. These normal brain MR images were compared with images of patients that suffered hypoxic-ischemic injury to determine the presence or absence of MR imaging abnormalities.

Thirty neonates aged 1 - 20 days (mean, 5.9 days) with HIE were identified. Fourteen of the neonates were female, and sixteen were male. MR imaging was performed six hours to 12 days (mean, 4.0 days) after the hypoxic-ischemic injury which included perinatal asphyxia (n = 24), neonatal seizure (n = 2), apnea (n = 2), and milk aspiration (n = 1). For this type of study, our institution did not require institutional review board approval.

MR imaging

MR imaging was performed using a 1.5 T MR scanner, either a Magnetom Vision (Siemens, Erlangen, Germany; n = 14) or a Magnetom Sonata (Siemens; n = 16). The following sequences were performed in all patients: axial T1-weighted imaging (time to repeat (TR) = 400 - 862 ms, time to echo (TE) = 12 - 20 ms), axial and coronal fast spin echo T2-weighted imaging (TR = 3140 - 7180 ms, TE = 90 - 117 ms) with fat suppression, axial fluid-attenuated inversion recovery (FLAIR) imaging (TR = 6000 - 9000 ms, TE = 100 - 119 ms, inversion time = 2500 ms), and axial diffusion-weighted imaging. In eight patients, axial gradient-echo (GRE) imaging (TR = 452 - 703 ms, TE = 15 - 26 ms, flip angle = 15 - 20 degrees) was also performed. The field of view (FOV), generally 105 - 150×120 - 160 mm, was adapted to the head size of the neonate. Other imaging parameters were as follows: section thickness, 3 - 5 mm; acquisition matrix, 256×256. Diffusion-weighted imaging was performed using an echo planar sequence with a 128×128 acquisition matrix, a 170 - 230×170 - 230 mm FOV, a 3 - 5 mm section thickness, and a b value of 0 and 1000 s/mm^2. Apparent diffusion coefficient (ADC) maps were obtained for all patients. Contrast-enhanced axial T1-weighted imaging was performed on 28 of 30 patients. For contrast studies, 0.2 mmol/kg gadopentate dimeglumine (Magnevist, Schering, Germany) was injected intravenously.

Lesion evaluation

One neuroradiologist and one radiologist, who did not participate in the process of the patient selection and were blinded to the specific clinical history, retrospectively compared the conspicuity of the HIE lesions on T1-weighted images, T2-weighted images, FLAIR images, and diffusion-weighted images, and determined which sequence demonstrated the highest lesion conspicuity for lesion detection. The most conspicuous sequences in different brain structures were then tabulat-

ed (Table 1). Disagreements regarding the findings were resolved by consensus. Brain structures were divided as follows: the cortex of both cerebral hemispheres; the white matter of both cerebral hemispheres; the deep gray matter; and the posterior limb of the internal capsule (12, 13); brain stem; and cerebellum. On GRE images that were obtained in eight patients, evidence of hemorrhage or calcification was evaluated. On post-contrast images, we determined whether contrast enhancement improved the lesion conspicuity. ADC maps were evaluated to verify a decrease of then ADC in hyperintense lesions on diffusion-weighted images.

Results

The results of qualitative analysis for lesion conspicuity and the patient characteristics are shown in Table 1. Table 2, which summarizes the findings of Table 1, shows the distribution of the most conspicuous MR sequences in different brain structures.

In the deep gray matter, T1-weighted images frequently depicted HIE lesions with greater conspicuity than diffusion-weighted images (9 of 14 patients, 64.3%)

Table 2. Distribution of the Most Conspicuous MR Sequences in the Different Brain Structures in 30 Neonates with HIE

Brain structures	T1	T2	FLAIR	DWI
Deep gray matter	9	0	1	4
Cerebral cortex	5	0	2	6
Cerebral white matter	0	0	4	16
PLIC	0	1	0	11
Brain stem	0	0	0	12*
Cerebellum	0	0	0	1†

Note: T1 = T1-weighted images; T2 = T2-weighted images; DWI = diffusion-weighted images.
* Eleven of the 12 patients had abnormal hyperintensity only in the corticospinal tract of the brain stem.
† Only cerebellar white matter was involved

Table 1. The Most Conspicuous MR Sequences in the Different Brain Structures and Clinical Data on 30 Neonates with HIE

Patient No.	Deep gray matter	Cerebral cortex	Cerebral white matter	brain stem	PLIC	cerebellum	GA (weeks-days)	Age of imaging (days)	Time after hypoxic ischemic injury (days)	Clinical history
1	-	-	D	-	-	-	36-5	7	2	Neonatal seizure
2	-	-	D	D	D	-	36-2	4	4	Perinatal asphyxia
3	-	F	F	D	D	-	36-1	6	6	Perinatal asphyxia
4	D	-	D	D	D	-	35-3	5	5	Perinatal asphyxia
5	-	-	F	-	-	-	38	14	12	Sudden apnea
6	T1	D	D	D	D	-	40-6	3	3	Perinatal asphyxia
7	F	F	-	D	D	-	39	9	9	Perinatal asphyxia
8	-	-	D	-	-	-	39-1	6	6	Perinatal asphyxia
9	T1	-	D	D	D	-	39-4	3	3	Perinatal asphyxia
10	-	-	D	-	-	-	37-1	1	1	Perinatal asphyxia
11	T1	T1	-	-	-	-	39	1	23 hours	Perinatal asphyxia
12	D	D	-	D	-	-	40-5	6	6	Perinatal asphyxia
13	T1	-	-	-	-	-	38-1	11	11	Perinatal asphyxia
14	-	-	F	-	-	-	38-3	6	6	Perinatal asphyxia
15	D	-	-	D	-	D	40-5	1	1	Perinatal asphyxia
16	D	D	D	-	-	-	39	1	1	Perinatal asphyxia
17	T1	-	F	-	D	-	38-1	6 hours	6 hours	Perinatal asphyxia
18	T1	-	D	-	-	-	37-4	8	4	Milk aspiration
19	-	-	D	D	D	-	38	2	2	Perinatal asphyxia
20	-	T1	D	D	D	-	40-3	7	7	Perinatal asphyxia
21	-	D	-	-	-	-	40	20	3	Sudden apnea
22	T1	D	D	D	-	-	38-4	4	4	Perinatal asphyxia
23	-	-	D	-	-	-	40-4	5	5	Perinatal asphyxia
24	T1	T1	-	-	T2	-	38-2	5	5	Perinatal asphyxia
25	-	T1	-	-	-	-	40-1	9	9	Perinatal asphyxia
26	-	-	D	-	-	-	39-4	5	20 hours	Neonatal seizure
27	T1	T1	D	D	-	-	38-3	4	4	Perinatal asphyxia
28	-	D	-	-	-	-	39-1	1	1	Perinatal asphyxia
29	-	-	-	-	D	-	40-4	1	1	Perinatal asphyxia
30	-	-	D	-	D	-	38-6	7	7	Perinatal asphyxia

Note: PLIC = posterior limb of internal capsule; GA = gestational age; T1 = T1-weighted images; F = fluid-attenuated inversion recovery images; T2 = T2-weighted images; D = diffusion-weighted images

(Figs. 1, 2). In the superficial gray matter (i.e., the cerebral cortex), T1- and diffusion-weighted imaging were similar for the number of the most conspicuous sequences (5/13 and 6/13, respectively) (Fig. 2).

In the white matter, the lesions were most conspicuous on diffusion-weighted images: lesions were detected in the cerebral white matter in 16/20 patients (80.0%), lesions were detected in the posterior limb of internal capsule in 11/12 patients (91.7%) and lesions were detected in the cerebellar white matter in one patient (100%) (Figs. 1, 3).

Twelve patients had an abnormally high signal in the brain stem as seen on diffusion-weighted images. In 11 of these 12 patients, only the corticospinal tracts were involved. These hyperintense lesions on diffusion-weighted images appeared as dark areas on the ADC maps.

On GRE images, which were obtained in eight patients, HIE lesions were less conspicuous than on any other sequence. The GRE images did not show characteristic dark signal foci, which suggested hemorrhage or calcification (Fig. 1). Contrast-enhanced T1-weighted images did not significantly improve the lesion conspicuity as compared with the pre-contrast T1-weighted images.

Discussion

In the deep gray matter, the HIE lesions were frequently depicted by T1-weighted images with greater conspicuity than with diffusion-weighted images. In the cerebral cortex, the usefulness of T1- and diffusion-weighted imaging for HIE lesion detection appeared to be comparable. The HIE lesions were revealed as hyperintense regions and were highlighted by the hypointense normal brain on T1-weighted images. These gray matter changes on T1-weighted images are consis-

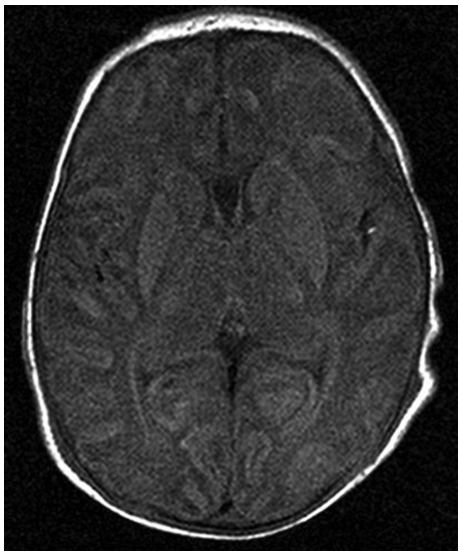

Fig. 2. Patient 27. A neonate of 38+3 week gestational age with perinatal asphyxia. Images at 4 days of age.
An axial T1-weighted image (TR/TE = 418/12) shows diffuse hyperintensity in the basal ganglia, lateral thalami, and cerebral cortex.

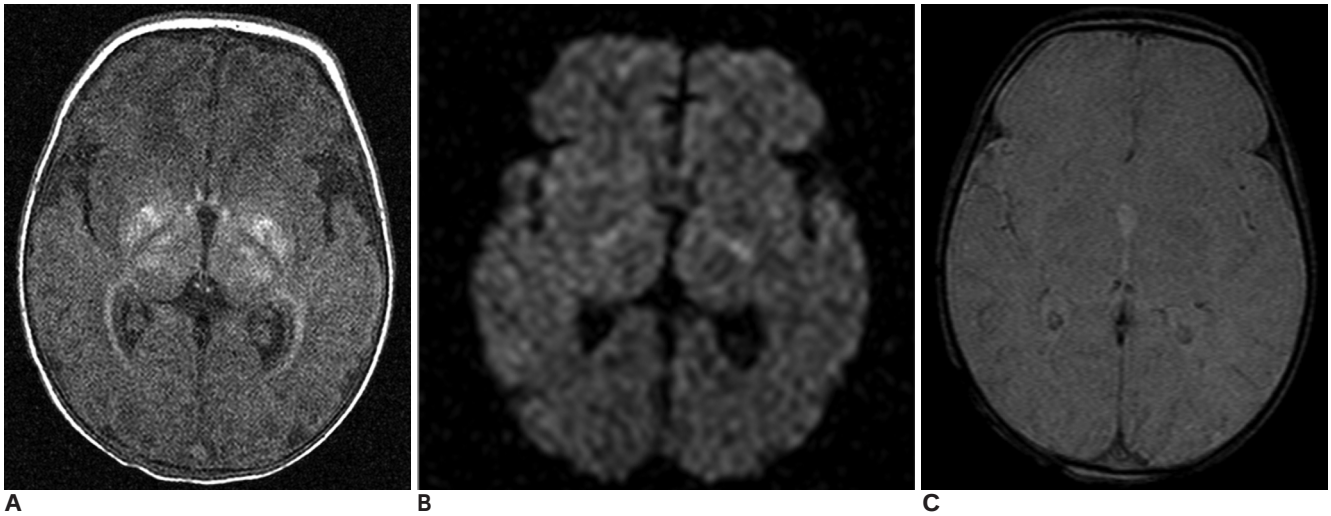

A **B** **C**

Fig. 1. Patient 17. A neonate of 38+1 week gestational age with perinatal asphyxia. Images at 6 hours of age.
A. An axial T1-weighted image (TR/TE = 418/12) shows abnormal hyperintensity in the posterior putamina and the lateral thalami.
B. An axial diffusion-weighted image at the same level as (**A**) shows hyperintensity in the posterior limbs of the bilateral internal capsules.
C. An axial GRE image (TR/TE = 608/15; flip angle = 15 degrees) at the same level as (**A**) and (**B**), does not show the characteristic dark signal which suggests hemorrhage or calcification in the hyperintense area on the T1-weighted image.

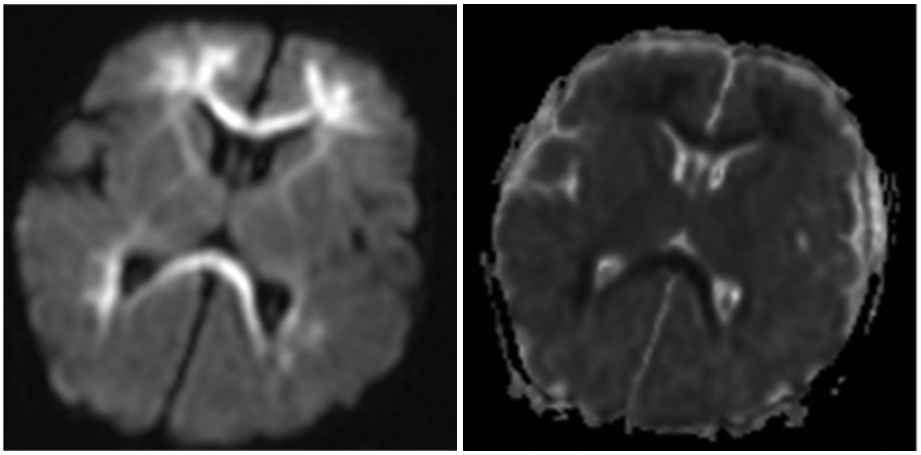

Fig. 3. Patient 30. A neonate of 38 + 6 week gestational age with perinatal asphyxia. Images at 7 days of age.
A. A diffusion-weighted image shows abnormal hyperintensity in the frontal white matter, peritrigonal white matter, internal capsules, and corpus callosum
B. An ADC map at the same level as (**A**) demonstrates a decreased ADC in the corresponding brain regions.

tent with the observations of previous reports (6, 14).

An interesting question is why the HIE lesions appear hyperintense on T1-weighted images. A number of factors can cause T1 shortening, resulting in hyperintensity on T1-weighted images. These factors include the following. (1) The interaction of water molecules with large surrounding molecules, as in a concentrated solution of protein (15), thus causing slowing of the water motion. (2) Lipids (16, 17). (3) Calcification (a surface relaxation mechanism) (18). (4) Paramagnetic compounds characterized by having at least one unpaired orbital electron (19) (a proton-electron spin-spin interaction), including products of hemorrhage, trace metals (e.g. manganese, copper, chromium, cobalt, and gadolinium) (20), molecular oxygen (O_2) (21), and free radicals (22). (5) High cellularity, e.g. a hamartoma and cortical laminar necrosis, for unknown reasons (23, 24). In the present study, petechial hemorrhage or hemorrhagic infarction seemed unlikely as a cause of the signal intensity of hemorrhagic brain tissue changes according to the process of hemoglobin degradation. GRE images obtained six hours and on 1, 2, 4, 5, 7, 9 and 12 days after hypoxic-ischemic insult in eight patients, demonstrated no evidence of hemorrhage. Moreover, in an autopsy study of eight neonates who died as a result of HIE (25), brain hemorrhage was not observed. The GRE images did not reveal evidence of calcification or metallic deposits. The ischemic lesions remained hyperintense on fat-suppressed, T2-weighted images. In addition, in view of the absence of the chemical shift artifact, the presence of a lipid is an unlikely cause of the signal intensity abnormality. Thus, hypercellularity and proton-electron interactions are possible causes of the hyperintensity of the HIE lesions on T1-weighted images.

Fujioka et al. reported similar MR imaging patterns in adults and rats who had sustained brief ischemia (26, 27). In patients with transient hemispheric ischemia caused by cardiogenic emboli, T1 hyperintensity in basal ganglia and cerebral cortex appeared on days 7 to 10 but not on days 2 to 3, and thereafter gradually faded away and disappeared. In addition, the affected structures atrophied over time during the period of the study. This ischemic change could be reproduced experimentally in rats after a 15-minute middle cerebral artery (MCA) occlusion. Selective neuronal death and gliosis were revealed in histological sections of the rat brain from the regions showing T1 hyperintensity (27). Although the histological examination revealed selective neuronal death and gliosis in the basal ganglia on days 3 and 7 after a 15-minute MCA occlusion, T1 hyperintensity did not appear on day 3. Therefore, Fujioka and colleagues speculated that the specific changes on T1-weighted images seemed to represent some biochemical changes that affect the magnetic field (27).

In a majority of our study patients, the white matter lesions were most conspicuous on diffusion-weighted images. These hyperintense lesions in the white matter on diffusion-weighted images appeared as dark areas on the ADC maps. However, diffusion-weighted imaging underestimated or failed to detect HIE lesions in the deep gray matter in many patients. With diffusion-weighted imaging, underestimation of the extent of disease or false-negative results were reported in demonstrating neonatal HIE lesions (7 - 11). Several explanations have been proposed to account for these false-negative results. However, those explanations do not appear to explain clearly the difference in the white versus the gray matter involvement as seen on diffusion-weighted images that was observed in the present study.

One of the explanations is a biphasic pattern of diffusion abnormalities which were observed previously in neonatal animal studies (28, 29). In neonatal rats, an initial reduction in the ADCs occurred at the end of hypoxia-ischemia. Upon re-oxygenation, the ADC returned transiently to normal, followed by a secondary decline 8 to 48 hours later. After this period, the ADC rose steadily. False-negative results and underestimation of diffusion-weighted imaging might have been caused by the transient recovery phase after the initial ADC decrease. Another explanation is "selective vulnerability" (10, 11). According to this premise, profound hypoxia-ischemia commonly causes damage in areas of high metabolic demand, such as the brain stem, the hippocampi, the basal ganglia, the thalami and the perirolandic cortex (6, 30). In contrast, less severe but more prolonged hypoxia-ischemic insults affect the cortical and subcortical watershed regions (6). Third, high water content in the neonatal brain (31) may also cause decreased sensitivity as seen on diffusion-weighted images (11, 32). While ischemia resulting in an area of decreased water diffusion is clearly seen in adults, the same decrease is relatively less pronounced in neonates and may not be easily discernible (11). Finally, apoptosis that is not detected using diffusion-weighted imaging may cause underestimation of the extent of disease or false-negative results in neonates with HIE (1, 33).

Our study results suggest that the pathophysiological response of the neonatal gray and white matter to ischemia differs. Studies of diffusion-weighted imaging and ADC changes in the neonatal white matter as compared with the gray matter are limited, and only two reports on ADC changes in the neonatal white matter after HIE could be found in the clinical literature (34, 35). Severely injured white matter demonstrated an ADC decrease, whereas in moderate lesions, the ADC was within the normal range (35). Mild injury caused an ADC increase in the white matter (34). These studies together indicate that ADC changes in the white matter appear to depend on the severity of HIE (34).

Overall, T2-weighted imaging was ranked lowest and the least useful in the present study. In neonates, the white matter is still in the process of myelination, and detection of ischemic changes is much more difficult on T2-weighted images (32). Moreover, it is known that HIE lesions show variable T2 hyper- or hypointensity (14). Therefore, estimating the extent of the injury would be difficult, even for the trained eye (32).

GRE imaging was performed in eight patients, but the GRE images did not show characteristic dark signal foci suggesting hemorrhage or calcification in any of these patients. Moreover, HIE lesions were less conspicuous on GRE images than on any other sequence. In the present study, conspicuity of the HIE lesions did not substantially increase following contrast administration. It seems that contrast enhancement does not have a significant effect on lesion conspicuity. Therefore, routine GRE imaging and contrast enhancement seem unnecessary in order to detect HIE lesions.

We did not perform quantitative analysis of the MR images in the present study. We considered that visual assessment was more useful in daily practice. Furthermore, Coskun et al. (36) reported that qualitative assessment is more predictive of the neuro-developmental outcome than quantitative analysis in neonates with HIE. Recently, Liauw et al. (37) have attempted develop a more objective method to identify HIE lesions on T1-weighted images. By comparing the signal intensities of different brain structures (the posterior limb of the internal capsule versus the posterolateral putamen and the corona radiata versus the perirolandic cortex) on T1-weighted images, only 65% (15/23) of infants with HIE were correctly predicted to have HIE. Their method does not seem to be satisfactory for detecting HIE lesions.

Conclusion

In summary, we compared the lesion conspicuity on T1-weighted images, T2-weighted images, FLAIR images, and diffusion-weighted images in neonates with HIE to determine which sequence demonstrated the highest lesion conspicuity for lesion detection. White matter lesions are the most conspicuous on diffusion-weighted images, whereas gray matter lesions show a tendency to have greater conspicuity on T1-weighted images than on the other MR sequences. T2-weighted imaging has a limited role in depicting HIE lesions. The routine use of GRE imaging and contrast enhancement seem unnecessary for the detection of neonatal HIE lesions.

Acknowledgements

A Pusan National University Research Grant supported this work for two years.

References

1. Grant PE, Yu D. Acute injury to the immature brain with hypoxia with or without hypoperfusion. *Radiol Clin North Am* 2006;44:63-77
2. Stoll BJ, Kliegman RM. *Hypoxia-ischemia*. In Behrman RE, Kliegman RM, Jenson HB. *Nelson Textbook of Pediatrics*. 17th ed. Philadelphia: WB Saunders, 2004;566-568
3. Hill A. Current concepts of hypoxic-ischemic cerebral injury in the term newborn. *Pediatr Neurol* 1991;7:317-325
4. Gieron-Korthals M, Colon J. Hypoxic-ischemic encephalopathy in infants: new challenges. *Fetal Pediatr Pathol* 2005;24:105-120
5. Aida N, Nishimura G, Hachiya Y, Matsui K, Takeuchi M, Itani Y. MR imaging of perinatal brain damage: comparison of clinical outcome with initial and follow-up MR findings. *AJNR Am J Neuroradiol* 1998;19:1909-1921
6. Barkovich AJ, Westmark K, Partridge C, Sola A, Ferriero DM. Perinatal asphyxia: MR findings in the first 10 days. *AJNR Am J Neuroradiol* 1995;16:427-438
7. Barkovich AJ, Westmark KD, Bedi HS, Partridge JC, Ferriero DM, Vigneron DB. Proton spectroscopy and diffusion imaging on the first day of life after perinatal asphyxia: preliminary report. *AJNR Am J Neuroradiol* 2001;22:1786-1794
8. Soul JS, Robertson RL, Tzika AA, du Plessis AJ, Volpe JJ. Time course of changes in diffusion-weighted magnetic resonance imaging in a case of neonatal encephalopathy with defined onset and duration of hypoxic-ischemic insult. *Pediatrics* 2001;108:1211-1214
9. Zarifi MK, Astrakas LG, Poussaint TY, Plessis Ad A, Zurakowski D, Tzika AA. Prediction of adverse outcome with cerebral lactate level and apparent diffusion coefficient in infants with perinatal asphyxia. *Radiology* 2002;225:859-870
10. Robertson RL, Ben-Sira L, Barnes PD, Mulkern RV, Robson CD, Maier SE, et al. MR line-scan diffusion-weighted imaging of term neonates with perinatal brain ischemia. *AJNR Am J Neuroradiol* 1999;20:1658-1670
11. Forbes KP, Pipe JG, Bird R. Neonatal hypoxic-ischemic encephalopathy: detection with diffusion-weighted MR imaging. *AJNR Am J Neuroradiol* 2000;21:1490-1496
12. Rutherford MA, Pennock JM, Counsell SJ, Mercuri E, Cowan FM, Dubowitz LM, et al. Abnormal magnetic resonance signal in the internal capsule predicts poor neurodevelopmental outcome in infants with hypoxic-ischemic encephalopathy. *Pediatrics* 1998;102:323-328
13. Hunt RW, Neil JJ, Coleman LT, Kean MJ, Inder TE. Apparent diffusion coefficient in the posterior limb of the internal capsule predicts outcome after perinatal asphyxia. *Pediatrics* 2004;114:999-1003
14. Chao CP, Zaleski CG, Patton AC. Neonatal hypoxic-ischemic encephalopathy: multimodality imaging findings. *Radiographics* 2006;26 Suppl 1:S159-S172
15. Daszkiewics OK, Hennel JW, Lubas B. Proton magnetic relaxation and protein hydration. *Nature* 1963;200:1006-1007
16. Fullerton GD. *Physiologic basis of magnetic relaxation*. In Stark DD, Bradley WG, Jr. *Magnetic Resonance Imaging*. 2nd ed. St Louis: Mosby Year Book, 1992;88-108
17. Mirowitz S, Sartor K. *Principles of examination and interpretation: image analysis and interpretation*. In Sartor K. *MR imaging of the Skull and Brain: A Correlative Text-Atlas*. New York, NY: Springer-Verlag, 1992;47-50
18. Henkelman RM, Watts JF, Kucharczyk W. High signal intensity in MR images of calcified brain tissue. *Radiology* 1991;179:199-206
19. Bradley WG, Jr. *Hemorrhage and brain iron: mechanism of proton relaxation enhancement*. In Stark DD, Bradley WG, Jr. *Magnetic Resonance Imaging* 2nd ed. St Louis: Mosby Year Book, 1992;722-728
20. Watson AD, Rocklage SM, Carvlin MJ. *Contrast agents: mechanisms of contrast enhancement*. In Stark DD, Bradley WG, Jr. *Magnetic Resonance Imaging* 2nd ed. St Louis: Mosby Year Book, 1992;374-377
21. Weinmann H-J, Gries H, Speck U. *Fundamental physics and chemistry: types of contrast agents*. In Sartor K. *MR imaging of the Skull and Brain: A Correlative Text-Atlas*. New York, NY: Springer-Verlag, 1992;26-28
22. Haimes AB, Zimmerman RD, Morgello S, Weingarten K, Becker RD, Jennis R, et al. MR imaging of brain abscesses. *AJR Am J Roentgenol* 1989;152:1073-1085
23. Barkovich AJ. MR and CT evaluation of profound neonatal and infantile asphyxia. *AJNR Am J Neuroradiol* 1992;13:959-972
24. Boyko OB, Burger PC, Shelburne JD, Ingram P. Non-heme mechanisms for T1 shortening: pathologic, CT, and MR elucidation. *AJNR Am J Neuroradiol* 1992;13:1439-1445
25. Jouvet P, Cowan FM, Cox P, Lazda E, Rutherford MA, Wigglesworth J, et al. Reproducibility and accuracy of MR imaging of the brain after severe birth asphyxia. *AJNR Am J Neuroradiol* 1999;20:1343-1348
26. Fujioka M, Taoka T, Hiramatsu KI, Sakaguchi S, Sakaki T. Delayed ischemic hyperintensity on T1-weighted MRI in the caudoputamen and cerebral cortex of humans after spectacular shrinking deficit. *Stroke* 1999;30:1038-1042
27. Fujioka M, Taoka T, Matsuo Y, Hiramatsu KI, Sakaki T. Novel brain ischemic change on MRI. Delayed ischemic hyperintensity on T1-weighted images and selective neuronal death in the caudoputamen of rats after brief focal ischemia. *Stroke* 1999;30:1043-1046
28. Rumpel H, Nedelcu J, Aguzzi A, Martin E. Late glial swelling after acute cerebral hypoxia-ischemia in the neonatal rat: a combined magnetic resonance and histochemical study. *Pediatr Res* 1997;42:54-59
29. Tuor UI, Kozlowski P, Del Bigio MR, Ramjiawan B, Su S, Malisza K, et al. Diffusion- and T2-weighted increases in magnetic resonance images of immature brain during hypoxia-ischemia: transient reversal posthypoxia. *Exp Neurol* 1998;150:321-328
30. Azzarelli B, Caldemeyer KS, Phillips JP, DeMyer WE. Hypoxic-ischemic encephalopathy in areas of primary myelination: a neuroimaging and PET study. *Pediatr Neurol* 1996;14:108-116
31. Neil JJ, Shiran SI, McKinstry RC, Schefft GL, Snyder AZ, Almli CR, et al. Normal brain in human newborns: apparent diffusion coefficient and diffusion anisotropy measured by using diffusion tensor MR imaging. *Radiology* 1998;209:57-66
32. Takeoka M, Soman TB, Yoshii A, Caviness VS, Jr., Gonzalez RG, Grant PE, et al. Diffusion-weighted images in neonatal cerebral hypoxic-ischemic injury. *Pediatr Neurol* 2002;26:274-281
33. D'Arceuil H, Rhine W, de Crespigny A, Yenari M, Tait JF, Strauss WH, et al. 99mTc annexin V imaging of neonatal hypoxic brain injury. *Stroke* 2000;31:2692-2700
34. Meng S, Qiao M, Scobie K, Tomanek B, Tuor UI. Evolution of magnetic resonance imaging changes associated with cerebral hypoxia-ischemia and a relatively selective white matter injury in neonatal rats. *Pediatr Res* 2006;59:554-559
35. Rutherford M, Counsell S, Allsop J, Boardman J, Kapellou O, Larkman D, et al. Diffusion-weighted magnetic resonance imaging in term perinatal brain injury: a comparison with site of lesion and

time from birth. *Pediatrics* 2004;114:1004-1014
36. Coskun A, Lequin M, Segal M, Vigneron DB, Ferriero DM, Barkovich AJ. Quantitative analysis of MR images in asphyxiated neonates: correlation with neurodevelopmental outcome. *AJNR Am J Neuroradiol* 2001;22:400-405
37. Liauw L, Palm-Meinders IH, van der Grond J, Leijser LM, le Cessie S, Laan LA, et al. Differentiating normal myelination from hypoxic-ischemic encephalopathy on T1-weighted MR Images: a new approach. *AJNR Am J Neuroradiol* 2007;28:660-665

대한영상의학회지 2008;58:97 - 104

신생아 저산소성 허혈성 뇌병증의 병변 명확도: 자기공명영상 연쇄간 비교[1]

[1]부산대학교병원 영상의학과
[2]부산대학교병원 소아청소년과

예대욱 · 김학진 · 김태언 · 남상욱[2] · 박수은[2]

목적: 저산소성 허혈성 뇌병증이 있는 신생아에서 병변의 명확도가 가장 높은 자기공명연쇄를 결정하고자 하였다.
대상과 방법: 저산소성 허혈성 뇌병증 신생아 30명에서 T1 강조, T2 강조, 액체감약반전회복, 확산강조 영상 간 병변의 명확도를 후향적으로 비교하였다. 뇌 구조물은 다음과 같이 나누었다: 대뇌 회질, 대뇌 백질, 심부 회질, 내포 후각, 뇌간, 소뇌.
결과: 심부 회질에서는 9/14(64.3%)명의 환자에서 T1 강조 영상이, 4/14 (28.6%)명에서는 확산 강조 영상이 다른 자기공명연쇄보다 병변을 명확하게 보여주었다. 대뇌 회질에서는 T1 및 확산강조영상의 명확도가 비슷했다 (각각 5/13, 6/13). 대부분 환자에서 백질 병변은 확산강조영상에서 병변의 명확도가 가장 높았다: 대뇌 백질 16/20 (80.0%), 내포 후각 11/12 (91.7%), 뇌간의 피질척수로 11/11 (100%), 소뇌 백질 1/1 (100%).
결론: 저산소성 허혈성 뇌병증이 있는 신생아에서 백질 병변은 확산강조영상에서 가장 명확하다. 그러나 회질 병변은 T1 강조영상에서 가장 명확하게 보이는 경우가 흔하다.